Design and Analysis of the High-Speed Underwater Glider with a Bladder-Type Buoyancy Engine

Dae-Hyeong Ji , Jung-Han Lee , Sung-Hyub Ko , Jong-Wu Hyeon , Ji-Hyeong Lee , Hyeung-Sik Choi , Sang-Ki Jeong *

Posted Date: 21 September 2023

doi: 10.20944/preprints202309.1390.v1

Keywords: underwater glider; buoyancy engine; resistance coefficients; horizontal speed; optimal glide angle

Article

Design and Analysis of the High-Speed Underwater Glider with a Bladder-Type Buoyancy Engine

Dae-Hyeong Ji [1], Jung-Han Lee [1], Sung-Hyub Ko [1], Jong-Wu Hyeon [1], Ji-Hyeong Lee [2,3], Hyeung-Sik Choi [4] and Sang-Ki Jeong [2,*]

[1] Marine Domain & Security Research Department, Korea Institute of Ocean Science and Technology, Busan, Republic of Korea
[2] Maritime ICT & Mobility Research Department, Korea Institute of Ocean Science and Technology, Busan, Republic of Korea
[3] Ocean Science and Technology School, Korea Maritime and Ocean University, Busan, Republic of Korea
[4] Department of Mechanical Engineering, Korea Maritime and Ocean University, Busan, Republic of Korea
* Correspondence: jeongs313@kiost.ac.kr; Tel: +8251-664-3045

Abstract: This study entailed the design and analysis of a 400 m-class underwater glider operated by a bladder-type buoyancy engine. The underwater glider was designed for high-speed movement with a maximum velocity of 2 knots. The shape of the hull was designed to reduce water resistance using the Myring hull profile equation. The reliability was verified by performing simulations using resistance coefficients. The relationship between the control value of the ballast discharged from the buoyancy engine and the glider's speed according to the path angle was analyzed. Further, the relationship between the optimal glide angle and the design control value of the ballast was derived, and the optimal glider speed was estimated accordingly. Based on the analysis results, a bladder-type buoyancy engine was developed, and the maximum speed of the tested underwater glider was measured via sea trials.

Keywords: underwater glider; buoyancy engine; resistance coefficients; horizontal speed; optimal glide angle

1. Introduction

In recent years, the discovery of marine resources has become a significant issue, as the world has been utilizing limited resources even in the face of energy shortages [1]. The ocean contains vast resources, including minerals and energy, a substantial part of which has remained underutilized. As the ocean has many life-threatening elements that are dangerous for humans, unmanned ocean exploration robots are essential for direct ocean exploration.

Autonomous underwater vehicles (AUV's) are well known as representative unmanned marine exploration robots. AUV's are underwater robots used for military and academic research because it can autonomously function with minimal operator intervention. AUV's collect various information about the marine environment and performs important missions such as surveillance and reconnaissance activities. This information can be used for exploration in the deep sea, which is particularly difficult for humans to access. However, as the propeller is used to generate propulsion, the hull would be heavy, and the volume would be large. In addition, as the amount of energy stored for generating propulsion is limited by the capacity of the battery, it is disadvantageous for long-term exploration. In contrast, underwater gliders (UG's) are unmanned marine exploration robots designed to travel between the ocean's depths and the ocean's surface, and their roles are not remarkably different from those of AUVs. Nevertheless, they are more efficient in terms of energy consumption because they do not use separate propellants [2]. The propulsive force in UG's is generated by buoyancy control by fluid inflow and outflow and by moment change using internal mass movement and wing movement. Therefore, they are suitable for long-time and long-distance ocean exploration because the power requirement is relatively small [2,3].

Preprints (www.preprints.org) | NOT PEER-REVIEWED | Posted: 21 September 2023 doi:10.20944/preprints202309.1390.v1

Currently, UG's are widely used in oceanographic research [4-6]. UG's can navigate by changing the ballast water amount in the buoyancy engine periodically such that it has good merit of using very small energy [7,8]. The dynamic models of UG's including the mass shifter motion were set up by a number of researchers [9-11]. There is also a study using back-stepping technology and direct adaptive control for UG's pitch control [12]. Various studies are also being conducted to reduce the tracking error of UG [13]. In addition, a UG that is less affected by ocean currents and has increased cruising speed is also being developed [14].

In this study, a UG capable of cruising at a maximum speed of 2 knots was designed according to the characteristics of the Korean peninsula. In addition, the payload in the middle of the hull is designed by increasing weight and buoyancy compared to the existing underwater glider so that various marine observation sensors can be mounted. The buoyancy engine of the UG was designed based on the purpose of operation, and the relationship between the control value of the ballast emitted from the buoyancy engine and the speed of the UG was analyzed. In addition, the reliability of the design was verified by performing dynamic modeling. After designing and manufacturing the UG system, we verified the maximum UG speed via sea trials.

In the following section, we first present the design and analysis of the hull of the UG. Section 3 introduces the mathematical model of the UG. Section 4 introduces the sea trials, and Section 5 presents a summary and conclusions.

2. Analysis of UG Hull

2.1. Hull shape design

The external design of the UG was designed using the Myring hull profile equations [15], which are empirical equations that can create an external shape that can minimize resistance from external fluids. The parameters used here are shown in Table 1. The bow and stern profile were designed using Equations (1) and (2):

$$\mathrm{r}(\Xi) = \frac{1}{2}d\left[1-\left(\frac{\Xi + a_{offset} - a}{a}\right)^2\right]^{\frac{1}{n}} \tag{1}$$

$$\mathrm{r}(\Xi) = \frac{1}{2}d - \left[\frac{3d}{2c^2} - \frac{\tan\theta}{c}\right](\Xi - l)^2 + \left[\frac{d}{c^2} - \frac{\tan\theta}{c}\right](\Xi - l_f)^3 \tag{2}$$

Table 1. Myring parameters for UG.

Parameters	Description	Units
a	Nose section length	m
a_{offset}	Nose offset	m
b	Constant radius center section length	m
c	Tail section length	m
c_{offset}	Tail offset	m
n	Exponential coefficient	-
θ	Included tail angle	radians
d	Maximum hull diameter	m
l	Vehicle total length	m
l_f	Vehicle forward length	m

The parameters used for the design are shown in Figure 1. By adjusting the parameters, a suitable shape can be obtained.

Preprints (www.preprints.org) | NOT PEER-REVIEWED | Posted: 21 September 2023 doi:10.20944/preprints202309.1390.v1

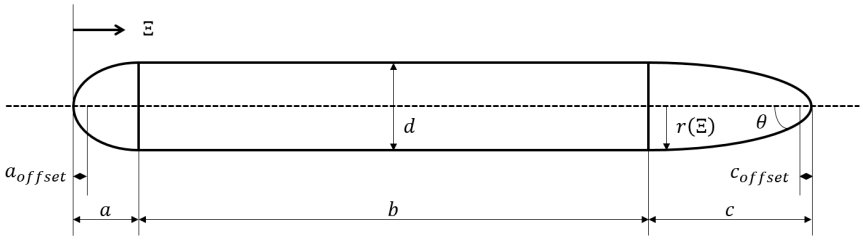

Figure 1. Myring equation parameters model.

2.2. Hull resistance analysis

Using computational fluid dynamics (CFD), the parameters related to the steering fluid force acting on the underwater glider were identified and used to estimate the kinetic performance of the UG at the design stage. The actual UG model designed for this purpose has a cylindrical shape with wings at a sweep angle of 20° attached to the oval regions at the fore and aft. For the analysis of turbulence, the k–ω SST model was applied. The flow velocity was analyzed with increasing velocity from approximately 0.2 m/s to 1.1 m/s. The flow velocity distribution around the UG decreases in the nose part and the curvature part of the thruster. The rear antenna and rudder were installed vertically based on these analysis results. The results of the resistance calculation for each speed obtained through the analysis are shown in Figure 2. All the results mentioned in this study were used in STAR-CCM+.

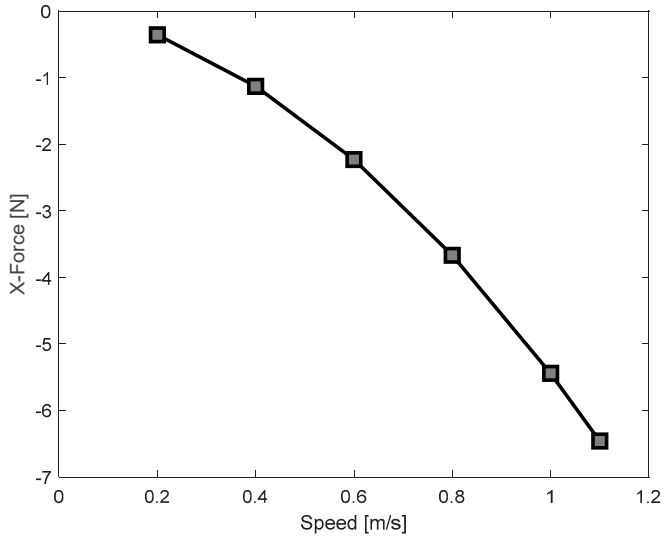

Figure 2. Relationship between speed and drag force.

A resistance of approximately 5.4 N acts when the UG moves straight at 1.0 m/s. Evidently, the resistance increases nonlinearly with speed, and the average drag coefficient calculated according to the obtained drag result is 0.29. Considering that the drag coefficient of an AUV with a torpedo-type hull is approximately 0.3, the calculated values are similar to those previously reported [16].

2.3. Maximum speed analysis

The ratio of lift and drag generated by the angle of attack(AoA) of the UG during gliding affects the stability of the pitching posture of the UG. As shown in Figure 3, when the angle of attack changes, the resultant force of lift and drag changes accordingly, and the posture of the UG needs to be corrected to achieve equilibrium.

Preprints (www.preprints.org) | NOT PEER-REVIEWED | Posted: 21 September 2023 doi:10.20944/preprints202309.1390.v1

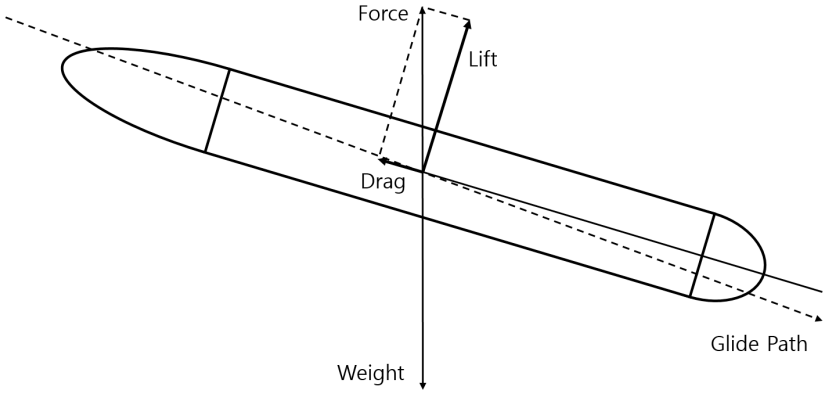

Figure 3. Action of lift and drag force.

As indicated by the CFD analysis results, Figure 4 summarizes the lift and drag coefficients according to the angle of attack. It was introduced in the performance optimization considering the part where the ratio of lift and drag is optimal during the glide of the UG. As shown in the figure, when the angle of attack of 0°–10° is considered, the increase in lift is more pronounced than the increase in drag.

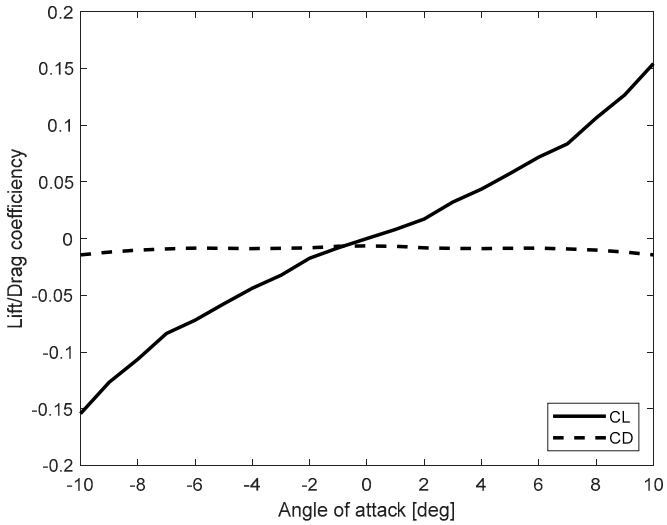

Figure 4. Simulated lift and drag coefficients.

The path angle of the UG can be expressed as shown in Equation (3) based on the ratio of lift and drag:

$$\zeta = -\tan\left(\frac{D}{L}\right) \tag{3}$$

Where, D is drag force, L is lift force, and ζ is glide path angle. Figure 5 shows the relationship between the angle of attack and the glide angle based on the calculated coefficients.

Preprints (www.preprints.org) | NOT PEER-REVIEWED | Posted: 21 September 2023 doi:10.20944/preprints202309.1390.v1

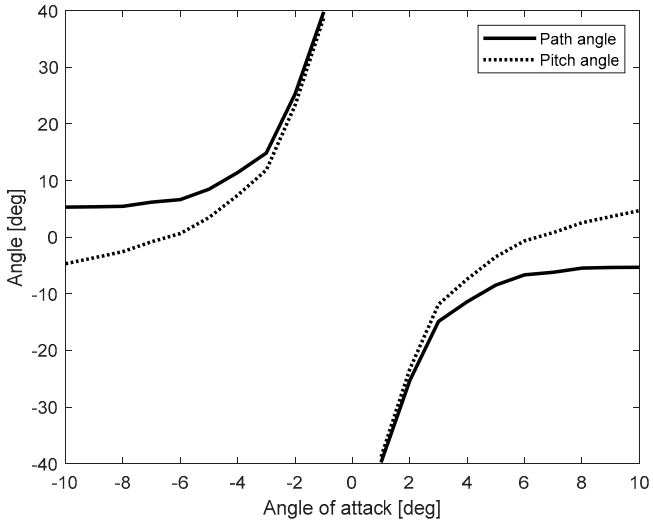

Figure 5. Relationship between the angle of attack and path angle.

The speed of the UG according to the maximum ballast control amount and the glide angle can be expressed by Equations (4), (5) and (6) [10]:

$$V = \left(\frac{m_0 g \sin\zeta}{\frac{1}{2}\rho C_D(\zeta(\alpha))} \right)^{1/2} \tag{4}$$

$$V_z = \left(\frac{m_0 g \sin\zeta}{\frac{1}{2}\rho C_D(\zeta(\alpha))} \right)^{1/2} \sin\zeta \tag{5}$$

$$V_x = \left(\frac{m_0 g \sin\zeta}{\frac{1}{2}\rho C_D(\zeta(\alpha))} \right)^{1/2} \cos\zeta \tag{6}$$

Where V is glide speed, V_Z is depth rate, V_X is horizontal speed, m_0 is excess mass, g is gravity, C_D is drag coefficient, ρ is density, α is angle of attack, and the calculation results are illustrated in Figure 6.

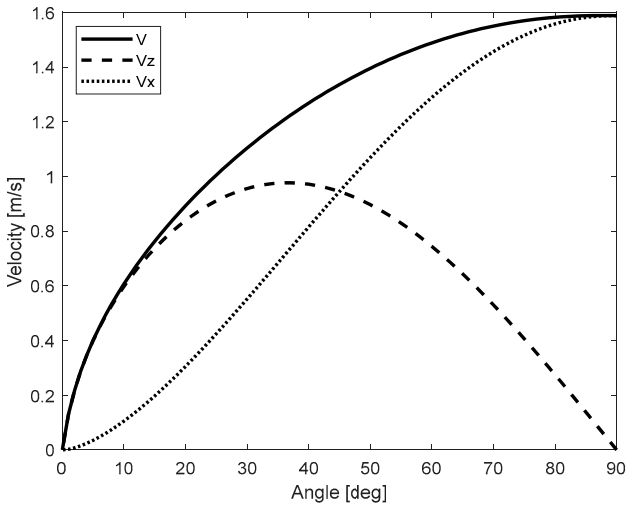

Figure 6. Relationship between glider velocity and path angle.

Preprints (www.preprints.org) | NOT PEER-REVIEWED | Posted: 21 September 2023 doi:10.20944/preprints202309.1390.v1

In Equation (4), the angle at which the horizontal speed (V_X) becomes the maximum is the point at which $\cos\zeta \sin^{1/2}\zeta$ is the maximum. As shown in Figure 7, the glide angle reaches its maximum at $\cos\zeta \sin^{1/2}\zeta = 0.657$ at 34°.

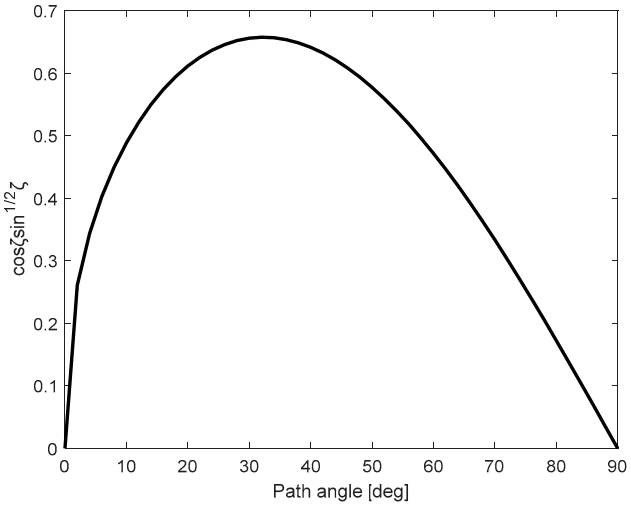

Figure 7. Relationship between $\cos\zeta \sin^{1/2}\zeta$ and path angle.

Equation (7) expresses the maximum speed of the UG as a function of the ballast control amount. The velocity relational expression based on the displacement and the maximum ballast control ratio ($n_b = m_0/\rho V$) was derived, and the relation is illustrated in Figure 8.

$$V_x = \left(\frac{m_0 g \sin\zeta}{\frac{1}{2}\rho C_D(\zeta(\alpha))} \right)^{1/2} \times 0.657 \tag{7}$$

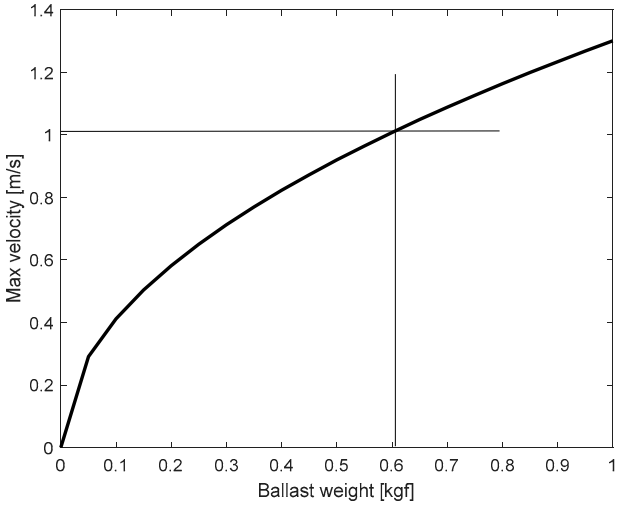

Figure 8. Relationship between maximum velocity and ballast water weight.

3. Mathematical Model of the UG

3.1. Structure of UG system

A photograph of the UG designed in this study is shown in Figure 10. The total weight of the UG is approximately 108 kg, the hull diameter is 280 mm, and the overall length is 2,200 mm. The hull was designed in a cylindrical shape to reduce water resistance. Inside, it consists of a buoyancy

Preprints (www.preprints.org) | NOT PEER-REVIEWED | Posted: 21 September 2023 doi:10.20944/preprints202309.1390.v1

engine, a posture controller, a battery, and a control device. The weight of the buoyancy engine can be increased for high-speed sailing, thereby increasing the overall weight of the hull. The detailed specifications of UG are shown in Table 2.

Figure 10. Developed UG.

Table 2. Specifications of UG.

Index	Value	Units
Length	2,200	mm
Diameter	280	mm
Width	1,450	mm
Height	348	mm
Weight	108	Kgf
Buoyancy	108	Kgf

3.2. Mathematical model of UG

The hull was assumed to be a rigid body to define the mathematical model of UG. The hull-fixed coordinate system and the earth-fixed coordinate system were used, as shown in Figure 11. The right-hand coordinate system with the forward direction as positive x, the starboard direction as positive y, and the vertically downward direction as the positive z direction was used. The translational and rotational motions about the UG's x, y, and z axes are expressed as six-degree-of-freedom (DOF) motions, and the coordinate axes and the motions are shown in Table 3.

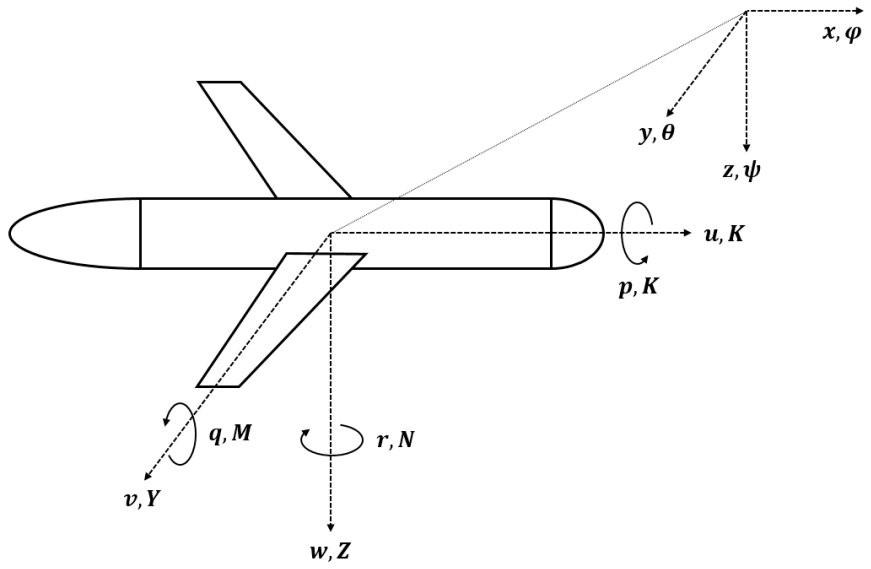

Figure 11. Coordinates frame of underwater glider.

Preprints (www.preprints.org) | NOT PEER-REVIEWED | Posted: 21 September 2023 doi:10.20944/preprints202309.1390.v1

Table 3. 6 DOF Motion of the underwater vehicle.

Classification	Axis	Motion	Fore & Moment	Velocity	Displacement
Translational motion	x	Surge	X	u	x
	y	Sway	Y	v	y
	z	Heave	Z	w	z
Rotational motion	x	Roll	K	μ	φ
	y	Pitch	M	q	θ
	z	Yaw	N	r	ψ

The equation of motion of the UG uses the six-DOF motion equation of a general submersible, as shown in Equations (8) [17]. The equations of motion are expressed in terms of forces and moments because of a significant number of hydrodynamic coefficients.

$$\begin{aligned}
&\mathrm{m}[\dot{u} - vr + wq - x_G(q^2 + r^2) + y_G(pq - \dot{r}) + z_G(pr + \dot{q})] = \mathrm{X} \\
&\mathrm{m}[\dot{w} - uq + vp - z_G(p^2 + q^2) + x_G(pq - \dot{r}) + y_G(pr + \dot{q})] = Z \\
&\mathrm{m}[\dot{w} - uq + vp - z_G(p^2 + q^2) + x_G(pq - \dot{r}) + y_G(pr + \dot{q})] = Z \\
&I_x\dot{p} + (I_z - I_y)qr + m[y_G(\dot{w} - uq + vp) - z_G(\dot{v} - wp + ur)] = K \\
&I_y\dot{q} + (I_x - I_z)rp + m[z_G(\dot{u} - vr + wq) - x_G(\dot{w} - uq + vp)] = M \\
&I_z\dot{r} + (I_y - I_x)pq + m[x_G(\dot{v} - wp + up) - y_G(\dot{u} - vr + wq)] = N
\end{aligned} \tag{8}$$

Here, u, v, w and p, q, r represents the UG angular velocity of translational and rotational motion for the axes x, y, z respectively. I_{ij} represent the mass moment of inertia of the UG for the axis of each subscript where x_G, y_G, z_G represent the location of the UG mass center. X, Y, Z, K, M, N represents the external forces and moment working on the UG for each motion direction such as thrust, buoyancy, gravity, and hydrodynamic force [18].

The external force term can be divided into the contributing forces, as shown in the following equations (9) and (10). Hydrostatic, inertial fluid, damping fluid, and control fluid forces, and respective moments result:

$$\sum F_0 = F_{hydrostatic} + F_{inertial} + F_{damping} + F_{control} \tag{9}$$

$$\sum M_0 = M_{hydrostatic} + M_{inertial} + M_{damping} + M_{control} \tag{10}$$

The following fluid force coefficients were obtained using empirical formulas for the hull shape of the designed underwater glider [16]. Substituting each coefficient into an external force component, Equation (11) result:

$$\begin{aligned}
&\mathrm{m}[\dot{u} - vr + wq - x_G(q^2 + r^2) + y_G(pq - \dot{r}) + z_G(pr + \dot{q})] \\
&\qquad = X_{HS} + X_{u|u|}u|u| + X_{\dot{u}}\dot{u} + X_{wq}\mathrm{wq} + X_{qq}qq + X_{vr}vr + X_{rr}rr \\
&\mathrm{m}[\dot{v} - wp + ur - y_G(r^2 + p^2) + z_G(qr - \dot{p}) + x_G(qp + \dot{r})] \\
&\qquad = Y_{HS} + Y_{v|v|}v|v| + Y_{r|r|}r|r| + Y_{\dot{v}}\dot{v} + Y_{\dot{r}}\dot{r} + Y_{ur}ur + Y_{wp}wp \\
&\qquad + Y_{pq}pq + Y_{uv}uv
\end{aligned} \tag{11}$$

Preprints (www.preprints.org) | NOT PEER-REVIEWED | Posted: 21 September 2023 doi:10.20944/preprints202309.1390.v1

$$\begin{aligned}&\mathrm{m}[\dot{w}-uq+vp-z_G(p^2+q^2)+x_G(pq-\dot{r})+y_G(pr+\dot{q})]\\&\qquad=Z_{HS}+Z_{w|w|}w|w|+Z_{q|q|}q|q|+Z_{\dot{w}}\dot{w}+Z_{\dot{q}}\dot{q}+Z_{uq}uq\\&\qquad+Z_{vp}vp+Z_{rp}rp+Z_{uw}uw\end{aligned}$$

$$\begin{aligned}&I_x\dot{p}+\left(I_z-I_y\right)qr+m[y_G(\dot{w}-uq+vp)-z_G(\dot{v}-wp+ur)]\\&\qquad=K_{HS}+K_{p|p|}p|p|+K_{\dot{p}}\dot{p}\end{aligned}$$

$$\begin{aligned}&I_y\dot{q}+(I_x-I_z)rp+m[z_G(\dot{u}-vr+wq)-x_G(\dot{w}-uq+vp)]\\&\qquad=M_{HS}+M_{w|w|}w|w|+M_{q|q|}q|q|+M_{\dot{w}}\dot{w}+M_{\dot{q}}\dot{q}+M_{uq}uq\\&\qquad+M_{vp}vp+M_{rp}rp+M_{uw}uw+M_{uu\delta_s}u^2\delta_s\end{aligned}$$

$$\begin{aligned}&I_z\dot{r}+\left(I_y-I_x\right)pq+m[x_G(\dot{v}-wp+up)-y_G(\dot{u}-vr+wq)]\\&\qquad=N_{HS}+N_{v|v|}v|v|+N_{r|r|}r|r|+N_{\dot{v}}\dot{v}+N_{\dot{r}}\dot{r}+N_{ur}ur+N_{wp}wp\\&\qquad+N_{pq}pq+N_{uv}uv+N_{uu\delta_r}u^2\delta_r\end{aligned}$$

The center of mass (r_G), mass moment of inertia (I_t), and center of buoyancy (r_B) change in real time owing to the movement of the internal mass and the buoyancy control device.

$$r_G(t)=\frac{m_h r_h+m_s r_s+m_m r_m(t)}{m_t} \tag{12}$$

Here m_t is the total mass of the UG, m_h is the mass of the external hull of the UG, m_s is the mass of the external hull of the UG and fixed components such as the internal control board and sensor module excluding the internal variable mass, and m_m represents the internal variable mass, respectively. r_h, r_s, r_m is the center of mass of the hull from the origin of the hull fixed coordinate system, and represents the position vectors from the center of mass of the fixed mass and the center of mass of the internal moving mass, respectively. In addition, the total mass moment of inertia of the underwater glider can be obtained as equation (13):

$$I_t(t)=(I_h-m_h\hat{r}_h\hat{r}_h)+(I_s-m_s\hat{r}_s\hat{r}_s)+\left(I_m-m_m\hat{r}_m(t)\hat{r}_m(t)\right) \tag{13}$$

Here, I_h, I_s, I_m represents the mass moment of inertia of the hull, the mass moment of inertia of the fixed mass, and the mass moment of inertia of the internal moving mass expressed at each center of mass. The operator ^ is an operator that converts a vector into a symmetric matrix to express the cross product of vectors.

$$I_t(t)=(I_h-m_h\hat{r}_h\hat{r}_h)+(I_s-m_s\hat{r}_s\hat{r}_s)+\left(I_m-m_m\hat{r}_m(t)\hat{r}_m(t)\right) \tag{14}$$

Here, V_{fix} represents the fixed volume of the submerged part of the UG at the stern side based on the y-z plane of the hull fixed coordinate system, $V_{var}(t)$ represents the volume of the submerged part of the UG on the bow side, which changes in real time according to the motion of the piston. And $V_t(t)$ represents the total volume of the UG submerged in water. $r_{var}(t)$ is the position vector from the origin of the hull fixed coordinate system to the center of the volume of the front part $V_{var}(t)$ and can be obtained through the position of the piston of the buoyancy control device that changes in real time. And r_{fix} represents the position vector of the rear part V_{fix} of the UG up to the center of the volume. By applying Equations (22), (23) and (24) to the nonlinear six-DOF motion equation, it is possible to describe the underwater motion of the glider according to the internal moving mass and buoyancy control [19].

Preprints (www.preprints.org) | NOT PEER-REVIEWED | Posted: 21 September 2023 doi:10.20944/preprints202309.1390.v1

4. Experiment

4.1. Gliding experiment

In this section, experiments were conducted in real waters to verify the movement speed derived from the design and modeling of the UG above. The test site was conducted in 1,000 m or more deep waters near Ulleungdo, South Korea. As for the experimental method, the results were confirmed after circumnavigating the UG once at a target depth of 250 m. When the UG floated to the surface after circumnavigating, it received internal measurement data through RF communication. Figure 12 shows the UG performing a circumnavigation experiment.

Figure 12. Gliding experiment of UG.

Figure 13 shows the water depth values obtained between UG circumnavigation. Approximately 300 s after the start of the experiment, the UG started submerging in the direction of the sea floor due to the change in buoyancy. At approximately 800 s, the buoyancy engine started to turn upward, and the change in water depth became gentle, and after reaching the maximum depth of approximately 260 m at 1,000 s, the hull started to float. It takes approximately 1,900 s to circumnavigate the depth of 260 m once.

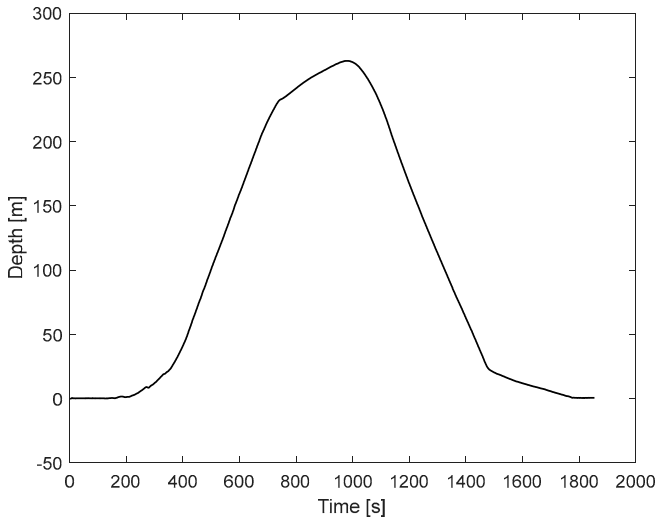

Figure 13. Depth result of UG while gliding.

Preprints (www.preprints.org) | NOT PEER-REVIEWED | Posted: 21 September 2023 doi:10.20944/preprints202309.1390.v1

Figure 14 shows that the UG controls the posture using the posture controller between circumnavigation. The previous speed analysis confirmed that the maximum moving speed was reached during circumnavigation at approximately 40°. Therefore, the pitch was controlled to ±40° during the circumnavigation. The target pitch was set to ±40° in consideration of the AoA at the angle derived from Figure 7. When diving, it was well controlled to the target value of -40°, and when ascending, the pitch was not controlled to +40° at the beginning and was controlled late. This seems to be a phenomenon that appears because the buoyancy control of the buoyancy engine takes some time.

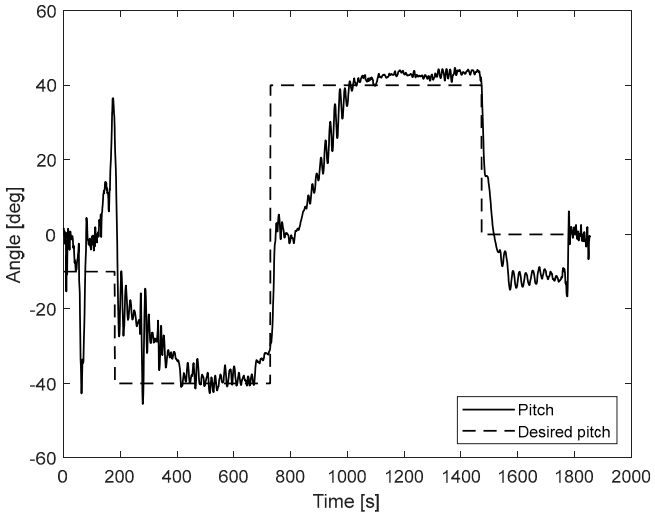

Figure 14. Pitch result of UG while gliding.

UG is sensitive to weight increase, and since it is a device that needs to minimize battery consumption, it cannot be equipped with a sensor such as DVL to measure speed. Therefore, the moving speed of the UG was calculated using a depth sensor and a digital compass, and the UG moving direction and sliding slope can be expressed as shown in Figure 15.

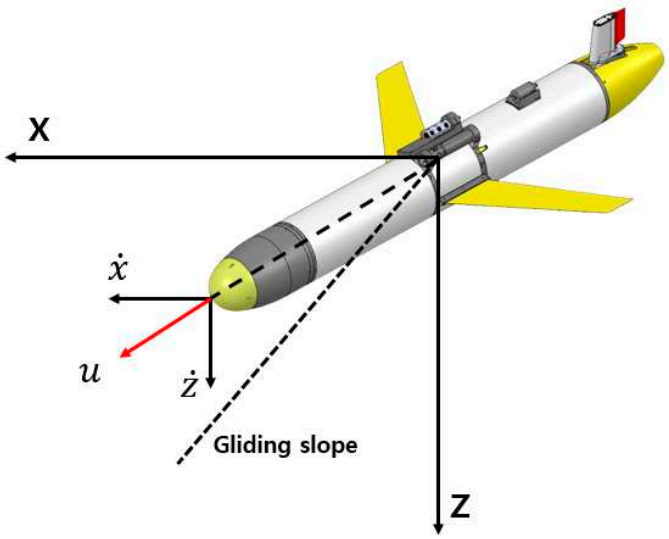

Figure 15. Coordinates frame of underwater glider.

The calculation of the moving speed in the moving direction of the UG can be expressed as Equation (15) below:

Preprints (www.preprints.org) | NOT PEER-REVIEWED | Posted: 21 September 2023 doi:10.20944/preprints202309.1390.v1

$$u = \frac{z_t - z_{t-s}}{-\sin(\theta \times \pi/180)} \quad (15)$$

Here, t is the current time, s is the sampling time, z is the depth, and θ is the pitch value. To simplify the movement speed calculation, only the pitch was considered in the posture drawing, and the absolute value of the pitch within 10° was calculated by substituting 0°.

Figure 16 shows the movement speed of UG calculated using Equation (15). It accelerated from approximately 300 s and achieved the maximum moving speed of 2.11 knots at 430 s. After maintaining approximately 1.8 knots until the upward transition, the movement speed increased again to approximately 1.5 knots after the movement speed fluctuated during the upward transition. At 1,500 s, it floated to the water, and the movement speed converged to almost 0 knots. The moving speed drops to a negative number in the 800–1,000 s section because the buoyancy engine's buoyancy control was slow. Thus, the motion change could not be accelerated except for the part where the motion of the UG changes (up-down transition), the average moving speed is confirmed to be 1 knot or more. According to the experimental results, similar to the results analyzed in the design, it was confirmed that the maximum moving speed of the UG was 2 knots or more, and high-speed circumnavigation was possible.

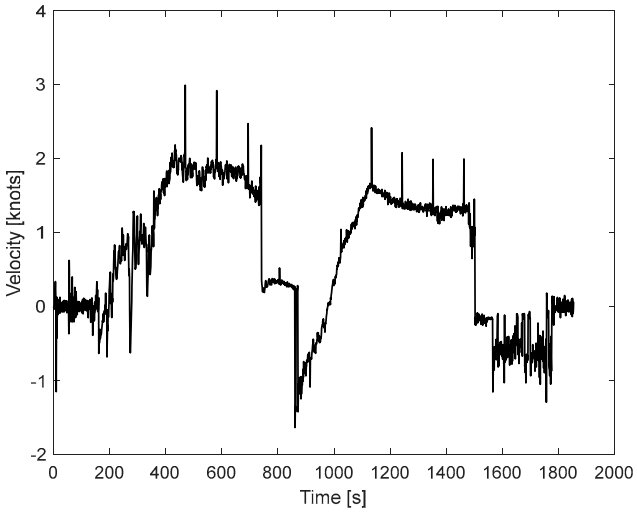

Figure 16. Velocity result of UG.

5. Conclusions

In this study, a UG capable of cruising at a maximum speed of 2 knots or more was designed and manufactured according to the characteristics of the Korean peninsula. The maximum movement speed of the UG was studied by comparing the mathematically calculated results with the actual sea area experimental results.

The steady-state motion in water was estimated by considering the lift force, and the buoyancy control capacity was calculated to obtain the target maximum moving speed of 2 knots. The submerged angle was calculated as 35°–40° from the circumnavigation trajectory to create the optimal motion state. In addition, the hull outline was designed using empirical formulas, and the reliability was secured by obtaining a resistance coefficient equivalent to that of the existing commercial underwater vehicle through CFD. Reliability was verified by simulating the behavior of UG through dynamic modeling by constructing a six-degree-of-freedom equation of an underwater body.

The movement speed of the UG was verified through the real sea area experiment. As a result of the experiment, it was confirmed that the maximum moving speed, 2.11 knots, was reached during submersion, and the average moving speed was over 1 knot except for the section where the motion was changed. According to the experimental results, similar to the results analyzed in the design, it

was confirmed that the maximum moving speed of the UG was 2 knots, and high-speed circumnavigation was possible.

In this study, the speed measurement sensor was not installed as a spatial constraint of the underwater glider. Therefore, a numerical calculation had to be performed to calculate the movement speed. In future studies, we will compare the results by preparing the speed measurement sensor.

Author Contributions: Conceptualization, D.-H.J. and H.-S.C.; methodology, S.-K.J.; software, D.-H.J. and S.-H.K.; validation, D.-H.J. and J.-W.H.; resources, J.-H.L.; data curation, D.-H.J.; writing—original draft preparation, D.-H.J.; writing—review and editing, S.-K.J. and H.-S.C.; supervision, S.-K.J.; project administration, J.-H.L.; funding acquisition, J.-H.L. All authors have read and agreed to the published version of the manuscript.

Funding: This research was supported by Unmanned Vehicles Core Technology Research and Development Program through the National Research Foundation of Korea(NRF) and Unmanned Vehicle Advanced Research Center(UVARC) funded by the Ministry of Science and ICT, the Republic of Korea(NRF-2020M3C1C1A02086324)

Institutional Review Board Statement: Not applicable.

Informed Consent Statement: Not applicable.

Data Availability Statement: Not applicable.

Conflicts of Interest: The authors declare no conflict of interest.

References

1. Shin, D.H.; Bae, S.B.; Baek, W.K.; Joo, M.G. Way-point tracking of AUV using Fuzzy PD controller. *Korea Institute of Information Technology* **2013**, *11*.
2. Park, J.J. Underwater glider: Its applicability in the East/Japan Sea. *Ocean and Polar Research* **2013**, *35*, 107-121.
3. Park, Y.-S.; Lee, S.-J.; Lee, Y.-K.; Jung, S.-K.; Jang, N.-D.; Lee, H.-W. Report of east sea crossing by underwater glider. *The Sea: JOURNAL OF THE KOREAN SOCIETY OF OCEANOGRAPHY* **2012**, *17*, 130-137.
4. Arima, M.; Tonai, H.; Kosuga, Y. Underwater glider 'SOARER'for ocean environmental monitoring. In Proceedings of the 2013 IEEE International Underwater Technology Symposium (UT), 2013; pp. 1-5.
5. Claus, B.; Bachmayer, R.; Cooney, L. Analysis and development of a buoyancy-pitch based depth control algorithm for a hybrid underwater glider. In Proceedings of the 2012 IEEE/OES Autonomous Underwater Vehicles (AUV), 2012; pp. 1-6.
6. Ruiz, S.; Renault, L.; Garau, B.; Tintoré, J. Underwater glider observations and modeling of an abrupt mixing event in the upper ocean. *Geophysical Research Letters* **2012**, *39*.
7. Sherman, J.; Davis, R.E.; Owens, W.; Valdes, J. The autonomous underwater glider" Spray". *IEEE Journal of Oceanic Engineering* **2001**, *26*, 437-446.
8. Yu, J.; Zhang, F.; Zhang, A.; Jin, W.; Tian, Y. Motion parameter optimization and sensor scheduling for the sea-wing underwater glider. *IEEE journal of oceanic engineering* **2013**, *38*, 243-254.
9. Bhatta, P.; Leonard, N.E. Nonlinear gliding stability and control for vehicles with hydrodynamic forcing. *Automatica* **2008**, *44*, 1240-1250.
10. Graver, J.G.; Leonard, N.E. Underwater glider dynamics and control. In Proceedings of the 12th international symposium on unmanned untethered submersible technology, 2001; pp. 1742-1710.
11. Isa, K.; Arshad, M.R. Dynamic modeling and characteristics estimation for USM underwater glider. In Proceedings of the 2011 IEEE Control and System Graduate Research Colloquium, 2011; pp. 12-17.
12. Nguyen, N.-D.; Choi, H.-s.; Jin, H.-S.; Huang, J.; Lee, J.-H. Robust Adaptive Depth Control of hybrid underwater glider in vertical plane. *Adv. Technol. Innov* **2020**, *5*, 135-146.
13. Jeong, S.-K.; Choi, H.-S.; Kang, J.-I.; Oh, J.-Y.; Kim, S.-K.; Minh Nhat, T.Q. Design and control of navigation system for hybrid underwater glider. *Journal of Intelligent & Fuzzy Systems* **2019**, *36*, 1057-1072.
14. Huang, J.; Choi, H.-S.; Jung, D.-W.; Lee, J.-H.; Kim, M.-J.; Choo, K.-B.; Cho, H.-J.; Jin, H.-S. Design and Motion Simulation of an Underwater Glider in the Vertical Plane. *Applied Sciences* **2021**, *11*, 8212.
15. Myring, D. A theoretical study of body drag in subcritical axisymmetric flow. *Aeronautical quarterly* **1976**, *27*, 186-194.
16. Prestero, T.T.J. Verification of a six-degree of freedom simulation model for the REMUS autonomous underwater vehicle. Massachusetts institute of technology, 2001.

17. Fossen, T.I. Guidance and control of ocean vehicles. University of Trondheim, Norway, Printed by John Wiley & Sons, Chichester, England, ISBN: 0 471 94113 1, Doctors Thesis **1999**.
18. Ji, D.-H.; Choi, H.-S.; Kang, J.-I.; Cho, H.-J.; Joo, M.-G.; Lee, J.-H. Design and control of hybrid underwater glider. *Advances in Mechanical Engineering* **2019**, *11*, 1687814019848556.
19. Kim, D.-H.; Lee, S.-S.; Choi, H.-S.; Kim, J.-Y.; Lee, S.-J.; Lee, Y.-K. Dynamic modeling and motion analysis of unmanned underwater gliders with mass shifter unit and buoyancy engine. *Journal of Ocean Engineering and Technology* **2014**, *28*, 466-473.